Surface albedo as a proxy for Greenland ice sheet ablation season mass balance*

William Colgan[1,2], Jason E. Box[1], Robert Fausto[1], Dirk van As[1],
Valentina R. Barletta[3], Xavier Fettweis[4], John Wahr[5,2] and R. Forsberg[3]

[1]Geological Survey of Denmark and Greenland, Copenhagen, Denmark
[2]Cooperative Institute for Research in Environmental Sciences, Boulder, USA
[3]Danish Technical University, Lyngby, Denmark
[4]University of Liège, Liège, Belgium
[5]University of Colorado, Boulder, USA

Originally posted online 17 June 2013
Revised (Version 2.1) 22 July 2013

* This interim supporting science document is based on a manuscript in preparation. The suggested citation for this work is: "Colgan, W., J. E. Box, R. Fausto, D. van As, V. R. Barletta, X. Fettweis, J. Wahr and R. Forsberg. in preparation. Surface albedo as a proxy for Greenland ice sheet ablation season mass balance."

1. Abstract

This study develops a first order method for filling gaps in the satellite gravimetry-derived record of monthly Greenland ice sheet mass balance. This method is based on a high correlation between gravimetry-derived ice sheet mass balance and ice sheet albedo during the May to September ablation season. Albedo conveniently integrates the competing surface mass balance effects of accumulation and ablation. We demonstrate that a single variable regression using satellite-observed monthly ice sheet albedo allows ice sheet mass balance to be estimated with essentially the same certainty as via satellite gravimetry during the ablation season (± 91 Gt/month). In the absence of satellite gravimetry observations, satellite-observed surface albedo therefore has utility as a first order proxy for ice sheet total mass balance. This albedo-mass balance regression can be employed with satellite-observed albedo to nowcast the Greenland ice sheet mass balance and provide monthly mass balance estimates two to three months before satellite gravimetry-derived estimates are available.

2. Introduction

Ice sheet mass balance exerts a significant influence on global mean sea level (e.g. Church and White, 2011; Gregory et al., 2012), thermohaline circulation (e.g. Fichefet et al., 2003; Rahmstorf et al., 2005), and ocean sediment nutrient influx (e.g. Rysgaard et al., 2003; Hasholt et al., 2006). With climate projections of increasing temperatures and ice sheet mass loss (Solomon et al., 2007), a likely global sea level rise of 1 m or more by century's end (Pfeffer et al., 2008) will come at massive infrastructural and livelihood costs. Remotely sensed observations, especially during the ablation season, are critical to understanding the response of Greenland ice sheet mass balance to contemporary climate change. The Gravity Recovery and Climate Experiment (GRACE) satellite constellation, launched in March 2002, provides monthly anomaly maps of Earth's gravity field. These monthly mass anomaly maps are valuable for observing mass fluxes, including regional mass change of ice sheets (Velicogna and Wahr, 2005; Luthcke et al., 2006). Data gaps have begun to appear more frequently in the GRACE temporal record (Greenland melt months June 2003, June 2011 and May 2012), due to a decline in the health of satellite batteries (http://podaac.jpl.nasa.gov/grace). While the GRACE constellation has already exceeded its five-year design lifetime by a factor of two, a follow-on satellite gravimetry mission is not scheduled to launch until after 2016.

In anticipation of further deteriorating temporal GRACE coverage, we present a regression-based approach, using mean monthly ice sheet wide surface albedo, to fill gaps in the GRACE-derived monthly record of total Greenland ice sheet mass change during the May to September period with greatest solar illumination and albedo variability. Surface albedo is examined as a predictor variable because it is readily observable and has documented accuracy (Stroeve et al., 2006; Box et al., 2012). Nowcasting a first order estimate of ice sheet mass balance appeals to both public interest in the health of the ice sheet, as well as researchers interested in the timely identification of extreme mass loss events. Surface albedo increases with fresh snowfall and decreases with increasing liquid water content during melt (e.g., Warren 1982; Lefebre et al., 2003; Hock, 2005). Albedo also varies predictably with near surface air temperature, due to the sensitivity of snow properties to available energy (Van As et al., 2013). Indeed, "ablation energy" has been inferred to be directly proportional to snow albedo (Konzelmann and Braithwaite, 1995). By virtue of these characteristics, ice sheet wide albedo exhibits a distinct annual cycle, reaching a minimum during the ablation season and a maximum during the winter accumulation season (Box et al., 2012), mirroring the annual cycle of ice sheet mass balance (e.g. Tedesco et al., 2013).

After introducing the gravimetry and surface albedo data sets employed by this study, we introduce the albedo-mass balance regression. We then assess the robustness of albedo as a proxy for Greenland ice sheet mass balance. We then discuss possible mechanisms that link ice flow dynamics with surface albedo on sub-monthly time scales, arguing that albedo may be regarded as a limited proxy for variability in dynamic mass. Finally, we present an application of the albedo-mass balance regression for nowcasting a first order estimate of Greenland ice sheet mass balance.

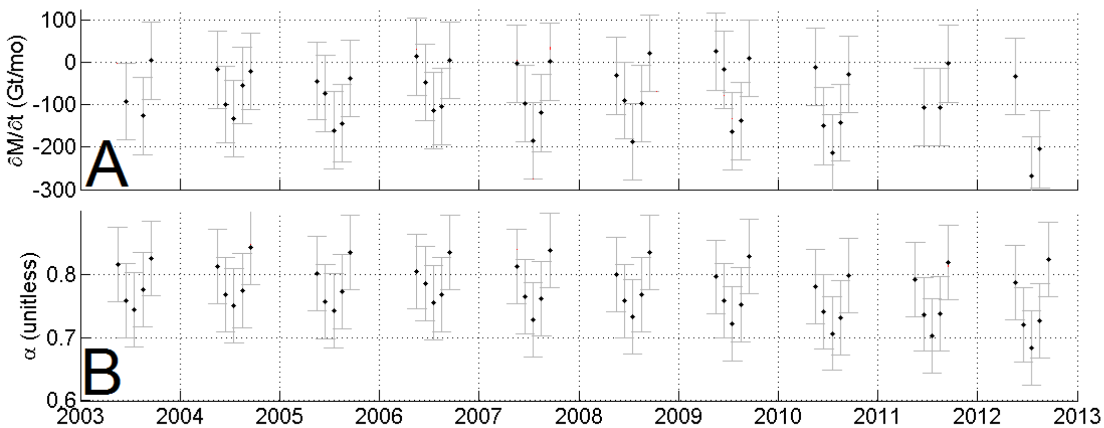

Figure 1: A: Ablation season (May to September) GRACE-derived monthly mass change (*∂M/∂t*; Barletta et al., 2012). **B:** MODIS-derived mean monthly ice sheet albedo (α; Box et al., 2012). Vertical bars correspond to each dataset's uncertainty as described in Section 3.

3. Data

3.1. GRACE

We assess ice sheet monthly mass change using updated Danish Technical University (DTU) monthly GRACE mass anomaly calculations after Barletta et al. (2012), which employ RL05 solutions from the 2003 through 2012 ablation seasons. Consistent with Hall et al., (2006), we take the ablation season to be the five-month period between 1 May and 30 September. We calculate the monthly rate of ice sheet mass change (*∂M/∂t* in Gt/month) using a node-centered finite difference of monthly GRACE mass anomalies (*M* in Gt):

$$\partial M/\partial t_2 = (M_3 - M_1)/(t_3 - t_1) \qquad \text{Eq. 1}$$

where t is time (in months), and subscripts 1, 2 and 3 denote consecutive months. The absolute uncertainty in the rate of ice sheet mass change calculated in this way is estimated as the quadratic sum of the uncertainties associated with both the M_1 and M_3 monthly mass anomaly solutions (Tedesco et al., 2013). The uncertainty in mass anomaly varies by month. DTU solutions have single standard deviation (1σ) monthly uncertainties ranging between 45 and 149 Gt, with an average of 91 Gt/month over the study period (Barletta et al., 2012). We take this average value as representative of the uncertainty in GRACE-derived monthly *∂M/∂t*.

As a consequence of using node-centered finite differencing, a single missing monthly GRACE mass anomaly solution prevents calculating monthly *∂M/∂t* according to Eq. 1 for the two months bounding the missing solution. For example, the missing June 2011 mass anomaly solution prevents calculating *∂M/∂t* for both

May and July 2011. DTU monthly gravity solutions are available for 46 of the 50 (or 92 %) months during the 2003 through 2012 ablation seasons (excluding June 2003, June 2011 or May 2012). Corresponding monthly *∂M/∂t* values calculated according to Eq. 1 are available for 44 of the 50 (or 88 %) ablation season months over the same period (not May/July 2003, May/July 2011 or June/September 2012; Fig. 1).

3.2. MODIS

Surface albedo retrievals from the NASA Terra platform Moderate-resolution Imaging Spectroradiometer (MODIS) sensor began in March 2000 (Hall et al., 2011). Only data from the Terra MODIS instrument are used here due to an Aqua MODIS instrument near infrared failure that reduces its cloud detection capability (Hall et al., 2008). Stroeve et al. (2006) demonstrated that the MOD10A1 product realistically captures the albedo annual cycle, but exhibits more temporal variability than in situ observations. A dominant component of this assessed error appears to be the failure of the MODIS data product to completely remove cloud effects. A possibly related problem is occasional spuriously low values, for example below 0.4 in the accumulation area, where ground observations indicate that albedo does not decrease below 0.7. We employ 11-day running statistics to identify and reject values that exceed 2σ from the mean. To prevent rejecting potentially valid cases, data within 0.04 of the median are not rejected (Box et al., 2012). Monthly averages are generated from these daily filtered data.

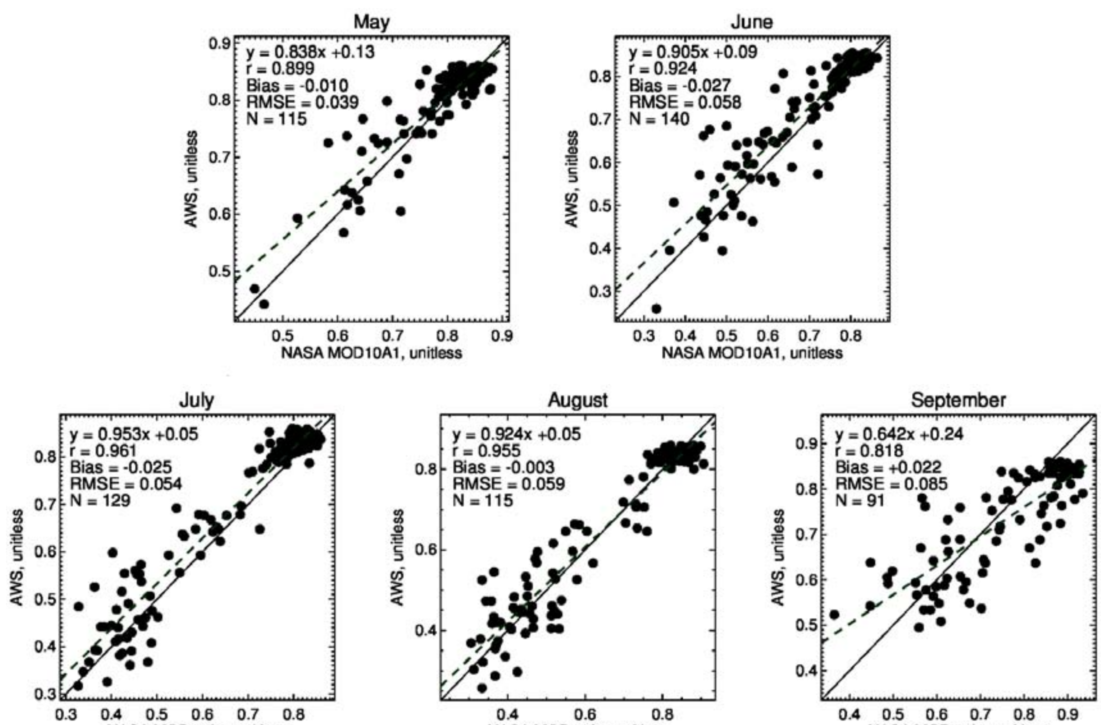

Figure 2: In situ surface albedo observed at PROMICE (Van As et al., 2013) and GC-Net (Steffen et al., 1996) automatic weather stations (where and when available) versus surface albedo remotely sensed by MODIS for all ablation season months since 2000. Solid line denotes zero bias (y = x), while the dashed line denotes an ordinary least squares regression in each month. The axes ranges differ between monthly subplots.

We assess the accuracy of MODIS MOD10A1 monthly average albedo during the ablation season by comparison with albedo observations from automatic weather stations (AWSs) operated by the Program for Monitoring of the Greenland ice sheet (PROMICE) (Van As et al., 2013) and the Greenland Climate Network (GC-Net; Steffen et al., 1996). The PROMICE network is located in the ablation area of the ice sheet, while GC-Net is located primarily in the accumulation area of the ice sheet. Relative to these in situ observations, we find the root mean squared error (RMSE) in MODIS albedo values reaches a minimum of 0.039 in May and a maximum of 0.085 in September (Fig. 2). We take the uncertainty associated with MODIS-derived mean monthly albedo as 0.059, which is the mean of monthly RMSE during the five-month ablation season (Fig. 1). Uncertainty in satellite-observed albedo increases substantially outside the ablation season (October to April), when solar illumination can be oblique or absent (Stroeve et al., 2006).

For a comparison, we obtain ice sheet wide mean monthly surface albedo over the 2000 through 2012 ablation seasons from the Modèle Atmosphèrique Régional (MAR) version 3.2 forced with ERA-Interim climate data (Fettweis et al., 2012). MAR is coupled with a one-dimensional multi-layered energy balance snow model (Gallée and Schayes, 1994; Lefebre et al., 2003), run with a horizontal resolution of 25 km, and forced every 6 hours at the lateral boundaries by the European Centre for Medium Range Weather Forecasts (ECMWF) ERA-Interim reanalysis (Dee et al., 2011). Although a high correlation exists between MAR and MODIS albedos for all months during the 2000 to 2012 period ($r = 0.932$, $p < 0.01$), the slope of the regression is only ~ 0.36 (Fig. 3), indicating that MAR systematically overestimates ice sheet wide surface albedo by up to 0.06 in comparison to MODIS, especially during relatively low albedo summer ablation season (Fig. 2). The MAR albedo bias likely results from modelled bare ice albedo values, which range between 0.4 and 0.6 depending on superficial meltwater presence (Lefebvre et al., 2003). In comparison, both in situ and MODIS observations suggest that the bare ice albedo in West Greenland can decrease below 0.3, or 25 to 50 % less than MAR modelled values (Box et al., 2012; Van As et al., 2013). Given the predominance of the West Greenland ablation area, this can result in a substantial MAR overestimation of ice sheet wide albedo during the ablation season. A solution to this source of bias may be implementing a background ice albedo field in MAR that is derived from MODIS imagery as in Van Angelen et al. (2012).

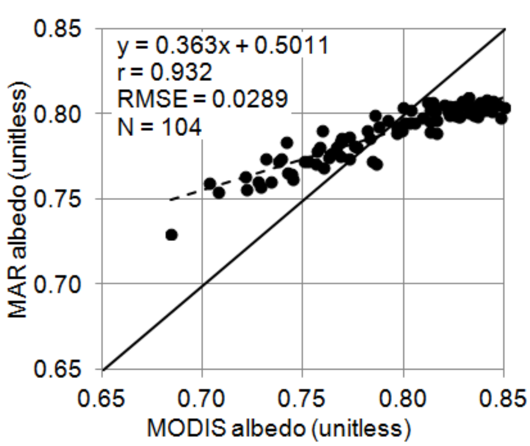

Figure 3: MAR version 3.2 (Fettweis et al., 2012) versus MODIS-derived (Box et al., 2012) mean monthly ice sheet albedo for all March to October months since March 2000. MAR systematically overestimates ice sheet wide surface albedo in comparison to MODIS during the relatively low albedo ablation season. Solid line denotes zero bias ($y = x$), while the dashed line denotes an ordinary least squares regression.

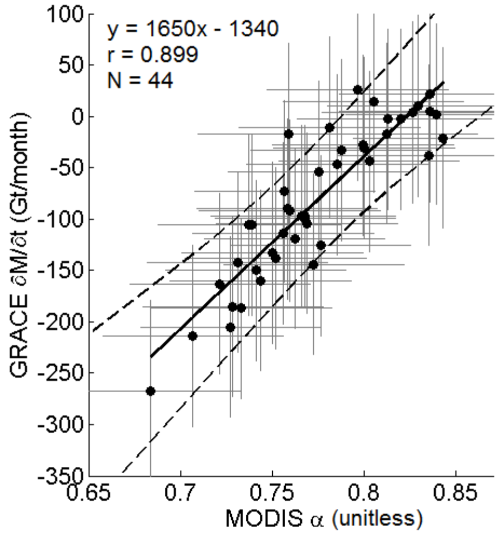

Figure 4: Ablation season (May to September) GRACE-derived monthly rate of mass change (*∂M/∂t*; Barletta et al., 2012) versus MODIS-derived mean monthly albedo (α; Box et al., 2012). Solid line denotes an ordinary least squares regression, while dashed lines denote a 2σ uncertainty envelope. Horizontal and vertical error bars denote uncertainty as described in Section 3.

4. Methodology

We evaluate a single variable regression model that employs monthly mean ice sheet albedo as a predictor for total ice sheet mass balance during the May to September ablation season. In comparison to interpolating missing monthly GRACE mass anomalies using a statistical approach, such as inserting average monthly observations (e.g. Tedesco et al., 2013), estimating monthly *∂M/∂t* values using a regression model based on a key climatic variable is nominally physically-based, in that it does not rely on a limited *∂M/∂t* history. MODIS-derived mean monthly albedo is strongly correlated with *∂M/∂t* over the five ablation season months during the 2003 to 2012 period ($r = 0.899$, $p < 0.01$; Fig. 4). This implies that ice sheet scale monthly *∂M/∂t* can be approximated by a linear albedo-mass balance regression of the form:

$$\partial M/\partial t = A\alpha + c \qquad \text{Eq. 2}$$

where α is the dimensionless MODIS-derived mean monthly surface albedo averaged over the entire ice sheet, *A* is a coefficient derived to equal 1650 ± 400 Gt/month, and *c* is a constant of -1340 ± 300 Gt/month. The ± uncertainty in these parameters represents their 1σ uncertainty when calculated over different temporal subsets of the 2003 to 2012 calibration period (see Section 5). *A* may be interpreted as representing the sensitivity of monthly *∂M/∂t* to albedo (i.e. a 0.01 decrease in mean monthly ice sheet albedo corresponds to 16.5 Gt decrease in monthly mass balance), while *c* may be interpreted as the theoretical maximum monthly *∂M/∂t* in the limit where the ice sheet absorbed all solar irradiance (e.g. α = 0). The minimum observed albedo at 5 km horizontal resolution is 0.29 (Box et al., 2012). Average ice sheet albedo for the June-August period for all Greenland ice has declined 6.4 % during the MODIS era (Fig. 5).

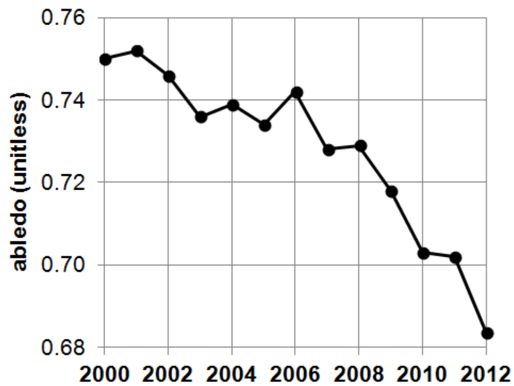

Figure 5: MODIS-derived June to August average Greenland ice sheet albedo (Box et al., 2012).

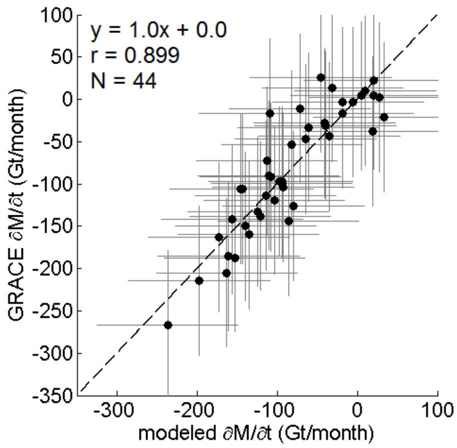

Figure 6: GRACE-derived monthly rate of mass change (*∂M/∂t*; Barletta et al., 2012) versus the *∂M/∂t* predicted by albedo regression using Eq. 2. Horizontal and vertical error bars denote ± 91 Gt/month as described in Section 5. Dashed line denotes zero bias (y = x).

5. Results

The monthly *∂M/∂t* values predicted by single variable albedo regression agree with the monthly *∂M/∂t* values observed by GRACE within an RMSE of ± 32 Gt/month ($r = 0.899$, $p < 0.01$; Fig. 6). We therefore suggest that in the absence of GRACE observations mean monthly surface albedo has utility as a first order proxy for total ice sheet scale mass balance. While this RMSE is approximately one third the uncertainty associated with finite differencing two monthly GRACE solutions to calculate a *∂M/∂t* value, we conservatively assume the uncertainty associated with the original GRACE *∂M/∂t* values as more representative of the absolute uncertainty associated with the albedo regressed *∂M/∂t* values (i.e. ± 91 rather than 32 Gt/month). Under this assumption, 98 % of the modelled versus observed *∂M/∂t* values lie within uncertainty of y = x (Fig. 6). To test if the relation between *∂M/∂t* and albedo is stationary in time, we evaluate the coefficient (*A*) and constant (*c*) of Eq. 2 for overlapping four-year intervals (e.g. 2003 to 2006, ... , 2009 to 2012) over the 2003 to 2012 GRACE record (Fig. 7). The values of *A* and *c* are indeed variable over subsets of the GRACE period. While the apparent increase in *A* over time is suggestive of a growing ice sheet mass balance sensitivity to albedo, the change is statistically insignificant (i.e. all *A* values are within their standard error of 1650 Gt/month). Until the GRACE record becomes long enough to derive significant trends in albedo sensitivity, albedo may be regarded as a temporally stationary proxy for mass balance over the observational period. Caution should be exercised if albedo were to be used as a first order proxy for mass balance beyond the observational record.

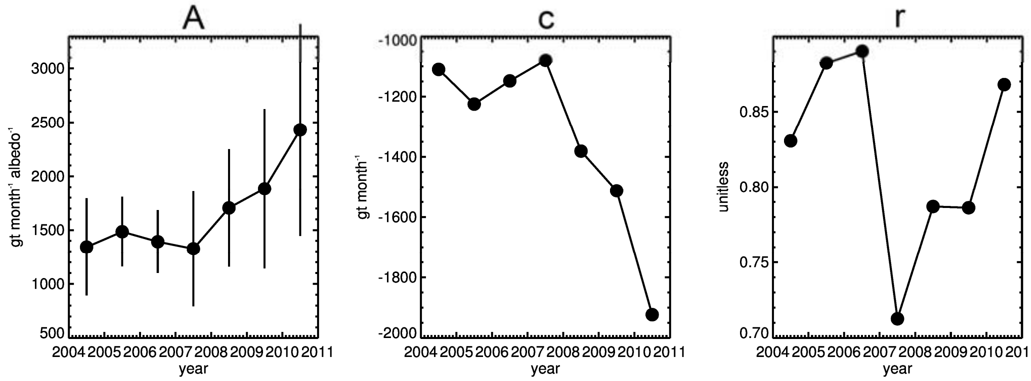

Figure 7: Evaluating coefficient (*A*), constant (*c*) and correlation (r) of the albedo-mass balance regression (Eq. 2) for overlapping four-year intervals (e.g. 2003 to 2006, 2004 to 2007, etc.) over the 2003 to 2012 GRACE period. Vertical lines denote slope standard error.

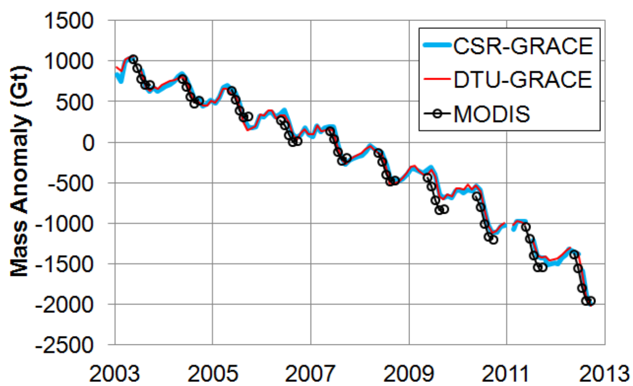

Figure 8: Cumulative mass anomaly observed by DTU and CSR GRACE solutions over the January 2003 to October 2012 period (Barletta et al., 2012; Tedesco et al., 2013), with cumulative MODIS albedo-derived mass balance shown for each ablation season.

Calculating cumulative MODIS-derived $\partial M/\partial t$ for each ablation season allows a qualitative comparison with DTU and Center for Space Research (CSR) GRACE mass anomaly time series (Barletta et al., 2012; Tedesco et al., 2013). This comparison shows that cumulative MODIS-derived $\partial M/\partial t$ captures the magnitude and rate of mass loss in each ablation season between 2003 and 2012 (Fig. 8). Calculating the residual between albedo and DTU GRACE-derived $\partial M/\partial t$ in each month permits a more quantitative assessment of the time-dependent mismatch between the two data series (Fig. 9). Albedo-regression appears to be biased towards overestimating mass loss early in the ablation season (i.e. -26 Gt/month on average in May and June), and biased towards underestimating mass loss late in the ablation season (i.e. +13 Gt/month on average in August and September). The absolute residuals between GRACE and albedo derived mass change are smallest in July, at the peak of the ablation season (18 Gt/month). The single largest residual is a mass loss overestimate of 92 Gt in June 2009. We speculate that this outlier is likely due to anomalously cold air temperatures following the initiation of spring melt, which resulted in both relatively low surface albedo and relatively low melt. National Centers for Environmental Prediction (NCEP) Reanalysis data suggests June 2009 was over 1 °C colder than the 1981 to 2010 climatic mean across all of Greenland (Kalnay et al., 1996). Similarly, at the seven out of thirteen PROMICE AWSs installed before June 2009, it was the coldest June recorded to date (Van As et al., 2013). In comparison, the albedo-derived mass loss residual of the July 2012 extreme melt month is 30 Gt, or approximately one third the uncertainty associated with finite differencing two monthly GRACE solutions.

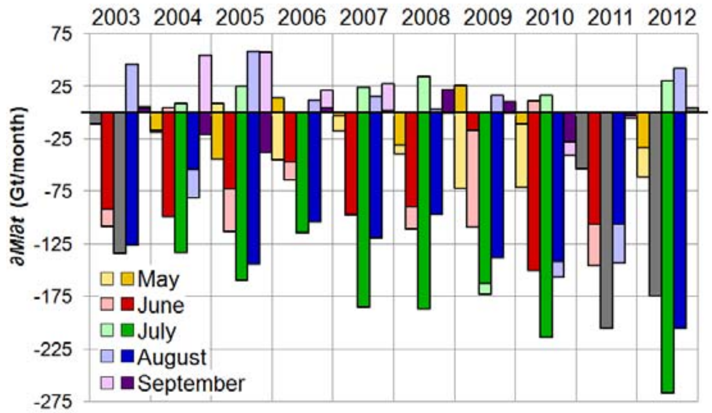

Figure 9: Monthly GRACE-derived mass change (dark shading; Barletta et al., 2012) and residual from the mass change estimated by albedo regression (light shading) over the 2003 to 2012 ablation seasons. Residuals below the x axis indicate an overestimation of mass loss by Eq. 2 and vice versa. Grey shading denotes when GRACE data is not available for comparison.

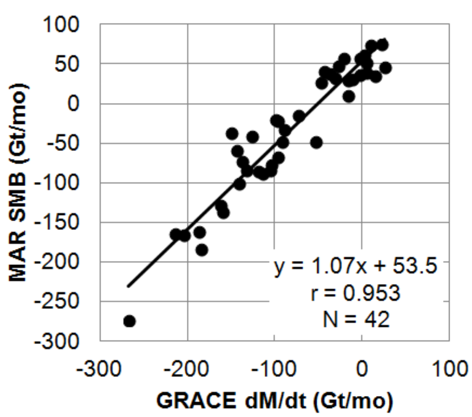

Figure 10: Monthly MAR-modelled surface mass balance (SMB; Fettweis et al., 2012) versus GRACE-derived mass balance (∂M/∂t; Barletta et al., 2012) during the May to September ablation season over the 2003 to 2012 period. Line denotes least squares regression.

6. Discussion

6.1. Ice sheet mass balance

The fidelity with which ice sheet wide surface albedo serves as a robust proxy for ice sheet mass balance suggests that surface mass balance plays a key role in influencing ice sheet mass balance. Indeed, the monthly surface mass balance derived from MAR version 3.2 forced with ERA-Interim climate data is highly correlated ($r = 0.953$, $p < 0.01$) with total ice sheet mass balance (as assessed by $\partial M/\partial t$ from Eq. 1) during the May to September ablation seasons over the 2003 to 2012 period (Fig. 10). We interpret the high correlation between MAR-modelled surface mass balance and GRACE-derived total mass balance as indicating that monthly *variability* in surface mass balance far exceeds monthly variability in ice flow during the ablation season. Ultimately, however, surface mass balance and ice dynamics interact. On decadal time scales surface mass balance variables such as runoff appear to serve as robust proxies for iceberg discharge (Box and Colgan, 2013).

Though MAR-modelled albedo systematically overestimates MODIS-observed albedo (Fig. 3), it is highly correlated with GRACE-derived mass balance ($r = 0.913$, $p < 0.01$; Fig. 11). We speculate that high correlation results from the one-dimensional multi-layered energy balance snow model implemented in MAR (Gallée and Schayes, 1994; Lefebre et al., 2003), which captures the radiative (solar and terrestrial), sensible and latent heat fluxes that all impact snow and ice melt, and accelerate snow crystal metamorphism, decreasing albedo. The sensible heat flux can approach 30 % of the solar flux over the Greenland ice sheet (Gallée and Duynkerke, 1997). We acknowledge that MAR-modelled surface mass balance is a better indicator of ice sheet mass balance than MODIS-observed albedo. Like GRACE-derived mass balance, however, MODIS-derived albedo is an observed, not modelled, ice sheet attribute. Unlike MAR-derived surface mass balance, obtaining MODIS-derived albedo does not require any ancillary climate data (i.e. substantial climate forcing data) and is available in real-time with minimal data processing.

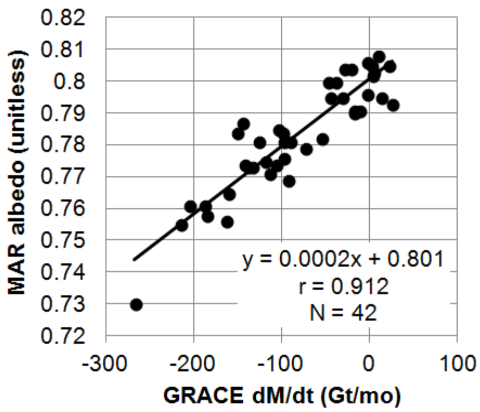

Figure 11: Monthly MAR-modelled surface albedo (Fettweis et al., 2012) versus GRACE-derived mass balance (dM/dt; Barletta et al., 2012) during the May to September ablation season over the 2003 to 2012 period. Line denotes least squares regression.

The physical basis for ice sheet albedo being a skilful predictor of $\partial M/\partial t$ is that albedo integrates the competing surface mass balance effects of accumulation and ablation, by albedo increasing with fresh snowfall and decreasing with increasing liquid water content during melt (e.g., Warren 1982; Lefebre et al., 2003; Hock, 2005). We postulate, however, that surface albedo is also expected to respond to changes in ice dynamics in a consistent fashion, whereby increasing dynamic mass loss decreases ice sheet albedo or a lower albedo results in higher dynamic mass loss. Below we describe five processes that directly link ice flow dynamics with ice sheet surface albedo on sub-monthly time scales.

(i) Tidewater destabilization: Lower albedos result in higher meltwater production due to a variety of surface mass balance processes increased solar radiation absorption (e.g. Box et al., 2012). On monthly time scales meltwater ejection at the underwater front of marine-terminating glaciers forces heat exchange between the glacier front and sea water (Motyka et al., 2011). Underwater melting undercuts the glacier front, promoting iceberg calving and reducing flow resistance. Thus, enhanced meltwater production (especially during low albedo ablation seasons) is expected to increase tidewater glacier discharge directly through underwater calving front destabilization.

(ii) Surface meltwater lakes: A relatively low albedo "dark zone" forms inland from the ice sheet margin each ablation season, where surface meltwater accumulation in supraglacial lakes reaches a maximum (Greuell, 2000). Sporadic rapid lake drainage enhances basal sliding on sub-monthly time scales by delivering large volumes of water to lubricate the ice-bed interface (e.g., Box and Ski, 2007; Das et al., 2008). During high melt years, Greenland surface meltwater lakes not only form further inland, at higher elevations, and are more likely to rapidly drain (Liang et al., 2012). Inter-annual variability in "dark zone" size is therefore proportional to enhanced basal sliding potential.

(iii) Bare ice area: The bare ice of the ablation area has a relatively low albedo in comparison to snow-cover. High melt years result in an upward migration of snow and firn lines, with a consequent increase in bare ice area (McGrath et al., 2013). Basal sliding is enhanced beneath relatively low albedo bare ice areas, in comparison to relatively high albedo snow- or firn-covered areas, due to: (i) an increase in meltwater runoff available to the glacier hydrology system, at the expense of a decrease in refreezing and retention in the near-surface snow and firn (Harper et al., 2012), and (ii) a decrease in the attenuation of meltwater pulses reaching the subglacial system, due to the absence of porous flow through snow or firn (Fountain and Walder, 1998).

(iv) Crevasse area extent: Heavily crevassed areas absorb twice as much solar radiation, and therefore have a nearly twice as low surface albedo compared to flat ice areas (Pfeffer and Bretherton, 1987). Changes in crevasse area have been observed to substantially modify glacier-averaged albedo on inter-annual timescales (Krimmel and Meier, 1975). A 13 ± 4 % increase in crevasse extent at Sermeq Avannarleq, West Greenland, since c. 1998 has been attributed to changes in ice geometry and flow direction due to the acceleration of nearby Jakobshavn Isbrae (Colgan et al., 2011). Increases in transient crevasse extent, due to increases in glacier velocity, are therefore expected to result in decreases in ice sheet surface albedo.

(v) Hydrofracture: The enhanced surface meltwater production during relatively low albedo periods results in an increase in meltwater supply and infiltration to existing surface crevasses and ice fractures. As a result of the density difference between water and ice, a continually filling surface crevasse can theoretically penetrate to the bed of the ice sheet via hydrofracture (Van der Veen, 1998). Hydrofracture is the wedging open of relatively low density ice by relatively high density water under the force of gravity. In addition to reducing the tensile strength of ice, which can enhance iceberg calving, the penetration of crevasses to the ice sheet bed has the potential to introduce abundant meltwater to the subglacial environment, where basal sliding can be enhanced on short (e.g. daily) time scales.

These albedo-dynamic processes not only influence the ice discharge of Greenland's outlet glaciers, but also the basal sliding of the ablation region as a whole, which varies on monthly time scales (Joughin et al., 2008a). We acknowledge that the primary link between albedo and ice sheet mass balance is undoubtedly surface mass balance. We merely highlight that these secondary links provide mechanisms by which albedo either influences, or is influenced by, the enhanced downstream conveyance of ice. Changes in terminus force balance due to buttressing (e.g. Joughin et al., 2008b), which also modulate ice dynamic mass loss a finite distance upstream from terminus (e.g. Colgan et al., 2012), are not directly linked to albedo.

6.2. Application: Nowcasting

The albedo regression presented in Section 4 can fill gaps in the GRACE observed record of May to September ice sheet mass balance. We use Eq. 2 to cautiously extend Greenland's ablation season $\partial M/\partial t$ record back three years to the year 2000 initiation of routine MODIS observation, and fill gaps in the more recent GRACE derived $\partial M/\partial t$ record (Fig. 12). As surface albedo is derived from readily available MODIS imagery, a first order surface albedo proxy for ice sheet mass balance potentially allows ice sheet mass balance to be quantitatively assessed, within given uncertainty, in near real time. By comparison, the direct assessments of ice sheet mass balance made by GRACE are subject to a significant time lag of at least two months, before variations in gravity can be translated into mass balance estimates (http://podaac.jpl.nasa.gov/grace). Indeed, real time albedo monitoring has already proven successful in qualitatively forecasting extreme negative mass balance years once the ablation season is underway (Box et al., 2012). Prior to reaching an absolute record low ice sheet wide albedo during the July 2012 extreme melt event, ice sheet wide albedo was already at the lowest observed on record in early June 2012.

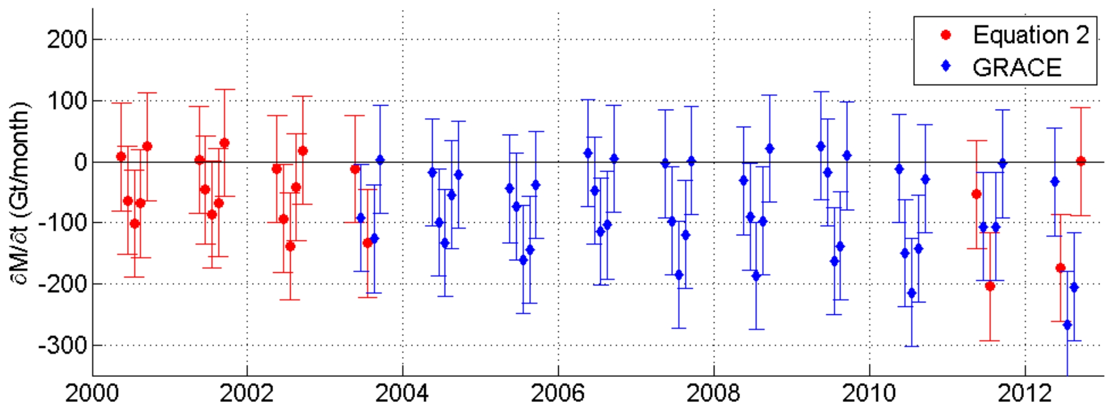

Figure 12: Ablation season (May to September) monthly rate of mass change (*∂M/∂t*) observed by GRACE (Barletta et al., 2012), and that predicted by albedo regression (Eq. 2), since 2000. Vertical error bars denote ± 91 Gt/month uncertainty as described in Section 5.

To provide a near real time estimate of ice sheet global sea level contribution, the Geological Survey of Denmark and Greenland (GEUS) has begun to interpret near real time MODIS MOD10A1 albedo data using the albedo-mass balance regression presented in Section 4. This permits GEUS to estimate a nowcast of ice sheet mass balance during the relatively short ablation season, two to three months before GRACE mass change solutions are available. During the ablation season (May to September) this nowcast of ice sheet mass balance has been updated weekly during the 2013 ablation season at www.polarportal.org. Nowcasting appeals to public interest in the health of the ice sheet, as well as scientists inclined to coordinate field campaigns to validate remotely sensed observations during extreme mass loss events (e.g. Nghiem et al., 2012)

Fig. 13 illustrates the nowcast web product of ice sheet sea level contribution estimated from both GRACE gravity solutions and MODIS MOD10A1 albedo data. To increase the accessibility of these technical products for public consumption, GRACE gravimetry-derived mass changes are referred to as "gravity estimates", while MODIS albedo-derived mass changes are referred to as "reflectivity estimates". Albedo-derived mass changes are computed from a daily time series of running monthly means. The top panel of the nowcast web product displays the instantaneous sea level rise contribution rate (in mm of global sea level equivalent per month), while the bottom panel displays the cumulative annual sea level contribution (in mm of global sea level equivalent). Monthly sea level contributions have 95 % confidence within a ± 0.196 mm sea level error margin. The 2003-2012 mean annual mass balance profile, as well as the 2012 extreme mass balance year, are also shown to place the current melt year in context.

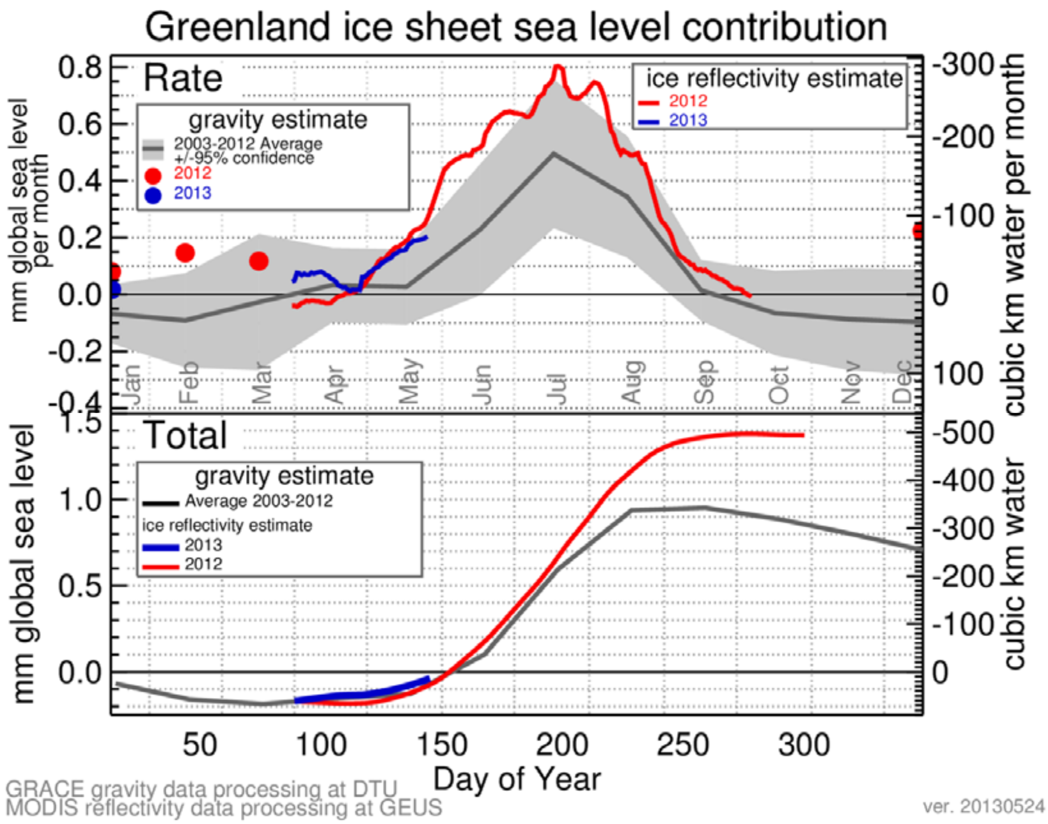

Figure 13: Greenland ice sheet instantaneous sea level rise contribution per month (**top**) and cumulative annual global sea level rise equivalent (**bottom**). Reflectively estimates are evaluated daily during the ablation season, while GRACE estimates are evaluated monthly throughout the year (when available). The 2003 to 2012 mean, and the 2012 extreme mass balance year, are included to place the current ablation season in context.

7. Conclusions

Deteriorating temporal GRACE coverage provides an impetus to explore a first order method for filling data gaps in the recent and future GRACE record. We explored a single variable regression to predict ice sheet mass balance as a function of mean monthly surface albedo. We find that this single variable regression allows monthly mass balance to be estimated with effectively the same uncertainty as GRACE derived estimates of monthly mass balance (i.e. ± 91 Gt/month). In the absence of GRACE observations, we therefore suggest that albedo has utility as a first order estimate for monthly ice sheet scale mass balance. We speculate that on the monthly time scale similar albedo-mass balance relations may also exist at basin-scale. We note that non-significant evidence of the albedo-mass balance regression being temporally non-stationary suggests that caution should be exercised when using albedo as a proxy for ice sheet mass balance outside the GRACE calibration period. We also note that surface albedo-derived mass balance is biased towards overestimating mass loss early in the ablation season (i.e. May and June) and underestimating mass loss late in the ablation season (i.e. August and September). These biases, however, are smaller (< 30 Gt/month) than the absolute uncertainty associated with calculating monthly mass balance from GRACE observations (91 Gt/month).

While we describe five processes that link surface albedo with ice dynamics (tidewater destabilization, surface meltwater lakes, bare ice area, crevasse area extent and hydrofracture), we acknowledge that the links between surface albedo and ice dynamics are indirect. Instead, we suggest that the relatively high correlation between albedo and mass balance highlights an important role of surface mass balance in modulating the mass balance of the Greenland ice sheet. The Geological Survey of Denmark and Greenland (GEUS) now employs MODIS surface albedo as a proxy for ablation season ice sheet mass balance using the methodology described in this paper. This allows the nowcasting of Greenland ice sheet monthly mass balance at www.polarportal.org, one to two months before GRACE mass change solutions are available.

8. Acknowledgements

This work is supported by the Programme for Monitoring of the Greenland Ice Sheet (PROMICE). W.C. received support from Danish Ministry of Science, Technology and Innovation award 11-115166.

9. References

Barletta, V., L. Sørensen and R. Forsberg. 2012. Variability of mass changes at basin scale for Greenland and Antarctica. The Cryosphere Discussions. 6: 3397-3446. doi:10.5194/tcd-6-3397-2012

Box, J.E. and W. Colgan. in press. Greenland ice sheet mass balance reconstruction. Part III: marine ice loss and total mass balance (1840-2010). Journal of Climate. doi: 10.1175/JCLI-D-12-00546.1

Box, J.E. and K. Ski. 2007. Remote sounding of Greenland supraglacial melt lakes: implications to sub-glacial hydraulics. Journal of Glaciology. 181: 257-265.

Box, J., X., Fettweis, J. Stroeve, M. Tedesco and D. Hall and K. Steffen. 2012. Greenland ice sheet albedo feedback: thermodynamics and atmospheric drivers. The Cryosphere. 6. doi:10.5194/tc-6-821-2012.

Church, J., and N. White. 2011. Sea-Level Rise from the Late 19th to the Early 21st Century. Surveys in Geophysics. 32: 585-602. doi: 10.1007/s10712-011-9119-1.

Colgan, W., K. Steffen, W. McLamb, W. Abdalati, H. Rajaram, R. Motyka, T. Phillips and R. Anderson. 2011. An increase in crevasse extent, West Greenland: Hydrologic implications. Geophysical Research Letters. 38. doi:10.1029/2011GL048491.

Colgan, W., H. Rajaram, R. Anderson, K. Steffen, H. Zwally, T. Phillips and W. Abdalati. 2012. The annual glaciohydrology cycle in the ablation zone of the Greenland ice sheet: Part 2. Observed and modeled ice flow. Journal of Glaciology. 58: 51-64. doi: 10.3189/2012JoG11J081.

Das, S., I. Joughin, M. Behn, I. Howat, M. King, D. Lizarralde and M. Bhatia. 2008. Fracture propagation to the base of the Greenland ice sheet during supraglacial lake drainage. Science. 320: 778-781.

Dee, D. P., Uppala, S. M., Simmons, A. J., Berrisford, P., Poli, P., Kobayashi, S., Andrae, U., Balmaseda, M. A., Balsamo, G., Bauer, P., Bechtold, P., Beljaars, A. C. M., van de Berg, L., Bidlot, J., Bormann, N., Delsol, C., Dragani, R., Fuentes, M., Geer, A. J., Haimberger, L., Healy, S. B., Hersbach, H., Hólm, E. V., Isaksen, L., Kållberg, P., Köhler, M., Matricardi, M., McNally, A. P., Monge-Sanz, B. M., Morcrette, J.-J., Park, B.-K., Peubey, C., de Rosnay, P., Tavolato, C., Thépaut, J.-N., and Vitart, F. 2001. The ERA-Interim reanalysis: configuration and performance of the data assimilation system. Quarterly Journal of the Royal Meteorological Society. 137: 553-597.doi:10.1002/qj.828, 2011.

Fettweis, X., B. Franco, M. Tedesco, J. van Angelen, J. Lenaerts, M. van den Broeke, and H. Gallée. 2012. Estimating Greenland ice sheet surface mass balance contribution to future sea level rise using the regional atmospheric climate model MAR. The Cryosphere Discussions. 6: 3101-3147. doi:10.5194/tcd-6-3101-2012.

Fichefet, T., C. Poncin, H. Goosse, P. Huybrechts, I. Janssens, and H. Le Treut. 2003. Implications of changes in freshwater flux from the Greenland ice sheet for the climate of the 21st century. Geophysical Research Letters. 30, 1911. doi:10.1029/2003GL017826.

Fountain, A., and J. Walder. 1998. Water flow through temperate glaciers. Reviews of Geophysics. 36: 299-328.

Gallée, H., and G. Schayes. 1994. Development of a three-dimensional meso-gamma primitive equation model: katabatic winds simulation in the area of Terra Nova Bay, Antarctica. Monthly Weather Reviews. 122: 671–685. doi:10.1175/1520-0493(1994)122.

Gallée, H., and P. Duynkerke. 1997. Air-snow interactions and the surface energy and mass balance over the melting zone of west Greenland during the Greenland Ice Margin Experiment. Journal of Geophysical Research. 102(D12): 13813-13824. doi:10.1029/96JD03358.

Gregory, J., N. White, J. Church, M. Bierkens, J. Box, M. van den Broeke, J. Cogley, X. Fettweis, E. Hanna, P. Huybrechts, L. Konikow, P. Leclercq, B. Marzeion, J. Oerlemans, M. Tamisiea, Y. Wada, L. Wake, and R. van de Wal. 2012. Twentieth-century global-mean sea-level rise: is the whole greater than the sum of the parts? Journal of Climate. doi:10.1175/JCLI-D-12-00319.1.

Greuell, W. 2000. Meltwater accumulation on the surface of the Greenland Ice Sheet: Effect on albedo and mass balance. Geografiska Annaler. 82: 489–498. doi:10.1111/j.0435-3676.2000.00136.x.

Hall, D. K., R. S. Williams, K. A. Casey, N. E. DiGirolamo, and Z. Wan. 2006. Satellite-derived, melt-season surface temperature of the Greenland Ice Sheet (2000-2005) and its relationship to mass balance. Geophysical Research Letters. 33. L11501. doi:10.1029/2006GL026444.

Hall, D. K., J. Box, K. Casey, S. Hook, C. Shuman, and K. Steffen. 2008. Comparison of satellite-derived and in-situ observations of ice and snow surface temperatures over Greenland. Remote Sensing of Environment. 112: 3739–3749. doi:10.1016/j.rse.2008.05.007.

Hall, D. K., G. Riggs, and V. Salomonson. 2011. MODIS/Terra Snow Cover Daily L3 Global 500m Grid V004, January to March 2003, Digital media, updated daily. National Snow and Ice Data Center, Boulder, CO, USA.

Harper, J., N. Humphrey, W. Pfeffer, J. Brown, and X. Fettweis. 2012. Greenland ice-sheet contribution to sea-level rise buffered by meltwater storage in firn. Nature. 491: 240-243.

Hasholt, B., N. Bobrovitskaya, J. Bogen, J. McNamara, S. Mernild, D. Milbourn, and D. Walling. 2006. Sediment transport to the Arctic Ocean and adjoining cold oceans. Nordic Hydrology. 37: 413-432.

Hock, R. 2005. Glacier melt: a review of processes and their modelling. Progress in Physical Geography. 29: 362-391.

Joughin, I., S. Das, M. King, B. Smith, I. Howat, and T. Moon. 2008a. Seasonal speedup along the western flank of the Greenland Ice Sheet. Science. 320: 781-783.

Joughin, I., I. Howat, M. Fahnestock, B. Smith, W. Krabill, R. Alley, H. Stern, and M. Truffer. 2008b. Continued evolution of Jakobshavn Isbrae following its rapid

speedup. Journal of Geophysical Research. 113: F04006. doi:10.1029/2008JF001023.
Kalnay, E., M. Kanamitsu, R. Kistler, W. Collins, D. Deaven, L. Gandin, M. Iredell, S. Saha, G. White, J. Woollen, Y. Jhu, M. Chelliah, W. Ebisuzaki, W. Higgins, J. Janowiak, K. Mo, C. Ropelewski, J. Wang, A. Leetmaa, R. Reynolds, R. Jenne, and D. Joseph. 1996. The NCEP/NCAR 4-Year Reanalysis Project. Bulletin of the American Meteorological Society. 77: 437-472.
Konzelmann, T. and R. Braithwaite. 1995. Variations of ablation, albedo and energy balance at the margin of the Greenland ice sheet, Kronprins Christian Land, eastern north Greenland. Journal of Glaciology. 41: 174-182.
Krimmel, R., and M. Meier. 1975. Glacier applications of ERTS images. Journal of Glaciology. 15: 391-402.
Lefebre, F., H. Gallée, J. van Ypersele and W. Greuell. 2003. Modeling of snow and ice melt at ETH Camp (West Greenland): A study of surface albedo. Journal of Geophysical Research. 108 (D8, 4231). doi:10.1029/2001JD001160.
Liang, Y., W. Colgan, Q. Lv, K. Steffen, W. Abdalati, J. Stroeve, D. Gallaher and N. Bayou. 2012. A decadal investigation of supraglacial lakes in West Greenland using a fully automatic detection and tracking algorithm. Remote Sensing of Environment. 123: 127-138.
Luthcke, S., H. Zwally, W. Abdalati, D. Rowlands, R. Ray, R. Nerem, F. Lemoine, J. McCarthy, and D. Chinn. 2006. Recent Greenland Ice Mass Loss by Drainage System from Satellite Gravity Observations. Science. 314: 1286-1289.
McGrath, D., W. Colgan, N. Bayou, A. Muto, and K. Steffen. 2013. Recent warming at Summit, Greenland: Global context and implications. Geophysical Research Letters. 40. doi:10.1002/grl.50456.
Motyka, R., M. Truffer, M. Fahnestock, J. Mortensen, S. Rysgaard, and I. Howat. 2011. Submarine melting of the 1985 Jakobshavn Isbræ floating tongue and the triggering of the current retreat. Journal of Geophysical Research. 116. F01007. doi:10.1029/2009JF001632.
Nghiem, S., D. Hall, T. Mote, M. Tedesco, M. Albert, K. Keegan, C. Shuman, N. DiGirolamo, and G. Neumann. 2012. The extreme melt across the Greenland ice sheet in 2012. Geophysical Research Letters. 39, L20502.
Pfeffer, W., and C. Bretherton. 1987. The effect of crevasses on the solar heating of a glacier surface. IAHS Publication. 170: 191-205.
Pfeffer, W., J. Harper, and S. O'Neel. 2008. Kinematic constraints on glacier contributions to 21st-century sea-level rise. Science. 321: 1340-1343. doi:10.1126/science.1159099.
Rahmstorf, S., M. Crucifix, A. Ganopolski, H. Goosse, I. Kamenkovich, R. Knutti, G. Lohmann, R. Marsh, L. Mysak, Z. Wang, and A. Weaver. 2005. Thermohaline circulation hysteresis: A model intercomparison. Geophysical Research Letters. 32, L23605. doi:10.1029/2005GL023655.
Rysgaard, S., T. Vang, M. Stjernholm, B. Rasmussen, A. Windelin, and S. Kiilsholm. 2003. Physical Conditions, Carbon Transport, and Climate Change Impacts in a Northeast Greenland Fjord. Arctic, Antarctic and Alpine Research. 35: 301-312.
Steffen, K., J. Box, and W. Abdalati. 1996. Greenland Climate Network: GC-Net. CRREL 96-27 Special Report on Glaciers, ice sheets and Volcanoes, tribute to M. Meier. edited by S. Colbeck. 98-103.
Stroeve, J.C., J.E. Box, and T. Haran. 2006. Evaluation of the MODIS (MOD10A1) daily snow albedo product over the Greenland ice sheet. Remote Sensing of Environment. 105: 155-171.
Solomon, S., D. Qin, M. Manning, R.B. Alley, T. Berntsen, N.L. Bindoff, Z. Chen, A. Chidthaisong, J.M. Gregory, G.C. Hegerl, M. Heimann, B. Hewitson, B.J.

Hoskins, F. Joos, J. Jouzel, V. Kattsov, U. Lohmann, T. Matsuno, M. Molina, N. Nicholls, J. Overpeck, G. Raga, V. Ramaswamy, J. Ren, M. Rusticucci, R. Somerville, T.F. Stocker, P. Whetton, R.A. Wood and D. Wratt. 2007. Technical Summary. In: Climate Change 2007: The Physical Science Basis. Contribution of Working Group I to the Fourth Assessment Report of the Intergovernmental Panel on Climate Change [Solomon, S., D. Qin, M. Manning, Z. Chen, M. Marquis, K.B. Averyt, M. Tignor and H.L. Miller (eds.)]. Cambridge University Press, Cambridge, United Kingdom and New York, NY, USA.

Tedesco, M., X. Fettweis, M. van den Broeke, R. van de Wal, C. Smeets, W. van de Berg, M. Serreze, and J. Box. 2011. The role of albedo and accumulation in the 2010 melting record in Greenland. Environmental Research Letters. 6. doi:10.1088/1748-9326/6/1/014005.

Tedesco, M., X. Fettweis, T. Mote, J. Wahr, P. Alexander, J. E. Box, and B. Wouters. 2013. Evidence and analysis of 2012 Greenland records from spaceborne observations, a regional climate model and reanalysis data. The Cryosphere. 7: 615-630.

van Angelen, J., J. Lenaerts, S. Lhermitte, X. Fettweis, P. Kuipers Munneke, M. van den Broeke, E. van Meijgaard, and C. Smeets. 2012. Sensitivity of Greenland Ice Sheet surface mass balance to surface albedo parameterization: a study with a regional climate model. The Cryosphere. 6: 1175-1186. doi:10.5194/tc-6-1175-2012.

van den Broeke, M., J. Bamber, J. Ettema, E. Rignot, E. Schrama, W. van de Berg, E. van Meijgaard, I. Velicogna, and B. Wouters. 2009. Partitioning Recent Greenland Mass Loss. Science. 326. doi:10.1126/science.1178176.

van As, D., R. Fausto, W. Colgan, J.E. Box and the PROMICE team. 2013. Darkening of the Greenland ice sheet due to the melt-albedo feedback observed at PROMICE weather stations. Geological Survey of Denmark and Greenland Bulletin. 28: 69-72.

van der Veen, C.J. 1998. Fracture mechanics approach to penetration of surface crevasses on glaciers. Cold Regions Science and Technology. 27: 31–47.

Warren, S. G. 1982. Optical-properties of snow. Reviews in Geophysics. 20: 67–89. doi:10.1029/RG020i001p00067.

Velicogna, I., and J. Wahr. 2005. Greenland mass balance from GRACE. Geophysical Research Letters. 32, L18505. doi:10.1029/2005GL023955.